Organic & Biomolecular Chemistry

Accepted Manuscript

This article can be cited before page numbers have been issued, to do this please use: X. Li, B. an, S. Zhang, J. Hu, T. Pan, L. Huang, C. Tang and A. S. C. Chan, *Org. Biomol. Chem.*, 2018, DOI: 10.1039/C8OB00875B.

ROYAL SOCIETY OF CHEMISTRY

rsc.li/obc

View Article Online
DOI: 10.1039/C8OB00875B

Design, synthesis and evaluation of selenium-containing 4-anilinoquinazoline hybrids as anticancer agents and the mechanism study

Baijiao An[1], Shun Zhang[1], Jinhui Hu[1], Tingting Pan[1], Ling Huang[1], Johnny Cheuk-on TANG[2,*], Xingshu Li[1,*] and Albert S. C. Chan[1]

School of Pharmaceutical Sciences, Sun Yat-sen University, Guangzhou 510006, China

State Key Laboratory of Chirosciences, Department of Applied Biology and Chemical Technology, The Hong Kong Polytechnic University, Hong Kong, P.R. China.

Abstract:

Inhibition of the tubulin polymerization represents one of the significant strategies in the treatment of cancer. Inspired by the excellent antitumor activity of EP128495 and the beneficial biological activities of selenium compounds, a series of new selenium-containing 4-anilinoquinazoline hybrids were synthesized and evaluated as tubulin polymerization inhibitors. The antiproliferative activities assay showed that most of compounds inhibited human sensitive cancer cells at low nanomolar concentrations. Mechanism study revealed that the optimal compound **5a** disrupted microtubule dynamics, decreased mitochondrial membrane potential and arrested Hela cells in the G2/M phase that finally resulted cellular apoptosis.

Introduction

Cancer is a major disease that seriously endangers human life and health.[1] With the rapid increase in the incidence of cancers worldwide, the existing drugs are far from to meet the needs. In cancer treatment, many single-target drugs play a crucial role in cancer therapy such as cisplatin, paclitaxel, and the kinase inhibitors. However, the complexity of carcinogenic mechanism, tumor heterogeneity and the emergence of drug resistance make

View Article Online
DOI: 10.1039/C8OB00875B

the treatment of cancer still a long way to go.[2-3] Among the various targets for the development of anticancer agents, tubulin polymerization or de-polymerization inhibitors has attracted a lot of attention as tubulin-microtubule systems play a critical role for a wide range of cellular processes.[4-8] Taxane and vinca alkaloids are the typical examples for the treatment of variety human cancer in the past decades.[9-10] Recetly, Cai et al. reported the discovery and evaluation of 2-chloro-N-(4-methoxyphenyl)-N-methylquinazolin-4-amine as a tubulin polymerization inhibitor, which exhibited highly activity in inducing of apoptosis and cell proliferation inhibition.[11]

Selenium (Se) is an essential trace mineral nutrient with multiple roles in human health,[12-13]

People living in low selenium areas are susceptible to selenium-related diseases such as Keshan disease,[14] Kashin-Beck disease,[15] and male infertility.[16] Thus, selenium compounds have attracted a vast interest in the last decades as promising chemo-preventive agents.[17-18] There are twenty-five selenoproteins in the human body that exert specific biological functions.[19] Seleno-cysteine (SeCys), which confers important functions in selenoprotein, may be replaced by cysteine (Cys) in the conditions of low Se status,[20] resulting in selenium-related diseases. One of the important functions of selenium compounds is antioxidant. It has been shown that selenium compounds exhibit antineoplastic properties by inhibiting the development of reactive oxygen species (ROS), thus protecting cells against oxidative DNA damage.[21] Because of the potential cancer therapeutic effects of Se, several organoselenium compounds have been developed for the inhibition of cancer cell growth in various xenograft rodent models for different cancers types, as well as to have synergistic effects in combination with chemotherapeutic drugs. [22-29]

In our previous work, we have reported the synthesis and evaluation of the selenium-containing compound, N,2-dimethyl-N-(4-(methylselanyl)phenyl)quinazolin-4-amine, and its analogues as anticancer agents.[30] It is well known that the minor modification of structure often leads to great changes in biological activity. In this paper, we report the design, synthesis and evaluation of 2-chloro-N-methyl-N-(4-selenocyanatophenyl)quinazolin-4-amine and its analogues as anticancer agents and the mechanism study.

View Article Online
DOI: 10.1039/C8OB00875B

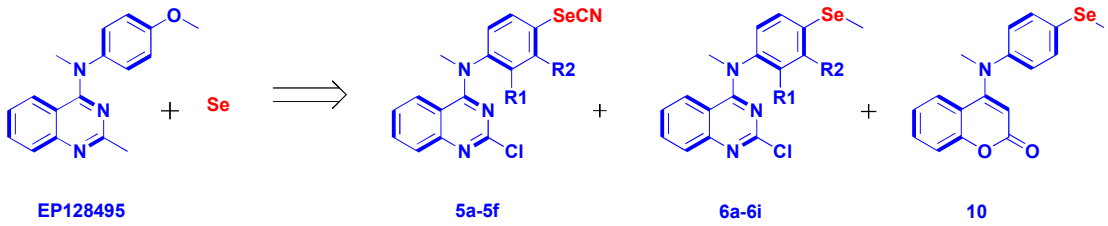

Figure 1. Design strategy of selenium-containing 4-anilinoquinazoline derivatives.

Results and discussion

Chemistry

The synthetic routes target compounds **5a, 5b, 5d, 5f, 6, 7a, 10** were outlined in Schemes 1-2. Commercially available starting materials substituted anilines (**1**) were reacted with paraformaldehyde in the solution CH_3ONa−CH_3OH and sequentially $NaBH_4$ to afford N-methylated compounds **2**. Treatment of **2** with malononitrile and SeO_2 in the solution of DMSO provided phenyl selenocyanate compounds **3**, which was reacted with $NaBH_4$ and CH_3I to afford the key intermediates **4a**, **4c**, **4e**, **4g**, **4h** and **4i**. Intermediates **3** were reacted with 2,4-dichloroquinazoline in the presence of hydrogen chloride in isopropanol to afford the target compounds **5a**, **5b**, **5d**, **5f**, which were further Se-methylated to give the target compounds **6a**, **6b**, **6d**, **6f**. Compounds **4** were reacted with 2, 4-dichloroquinazoline in the presence of NaOAc or NaH to give the target compounds **6a**, **6c**, **6e**, **6g**, **6h** and **6i**. The chloride on the 2-position of quinazoline moiety of **6a** was substituted by OCH_3 in the presence of NaOH and CH_3OH to afford **7a**. Target compounds **10** was synthesized by the reaction of 4-hydroxy coumarins (**8**) with P_2O_5 and Bu_4NBr in toluene to get intermediate **9**, which was coupled with 2, 4-dichloroquinazoline in the presence of DIEPA in DMF at 110°C for 12 hours.

View Article Online
DOI: 10.1039/C8OB00875B

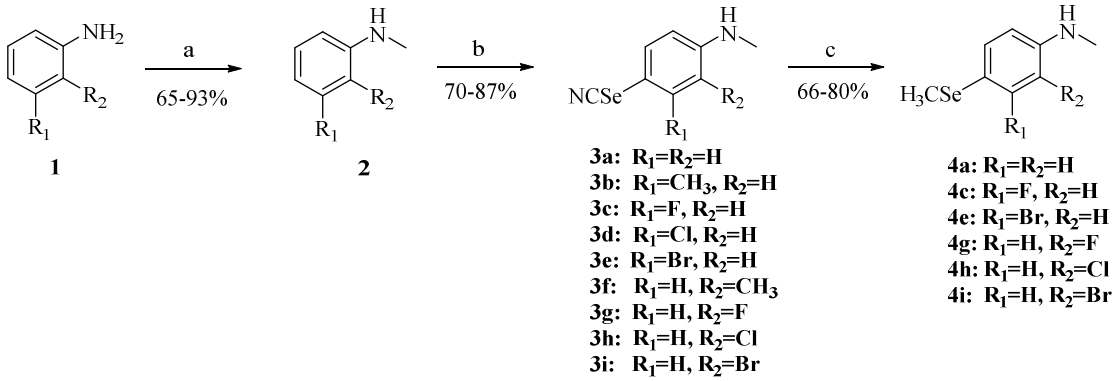

Scheme 1. The synthesis of intermediates **3** and **4**. Reagents and conditions: (a) i: Na, paraformaldehyde, CH_3OH, 12h, 0°C. ii: $NaBH_4$, 2h, 60°C. (b) Malononitrile, SeO_2, DMSO, 2h, r.t. (c) $NaBH_4$, CH_3I, CH_3OH, 5min, r.t.

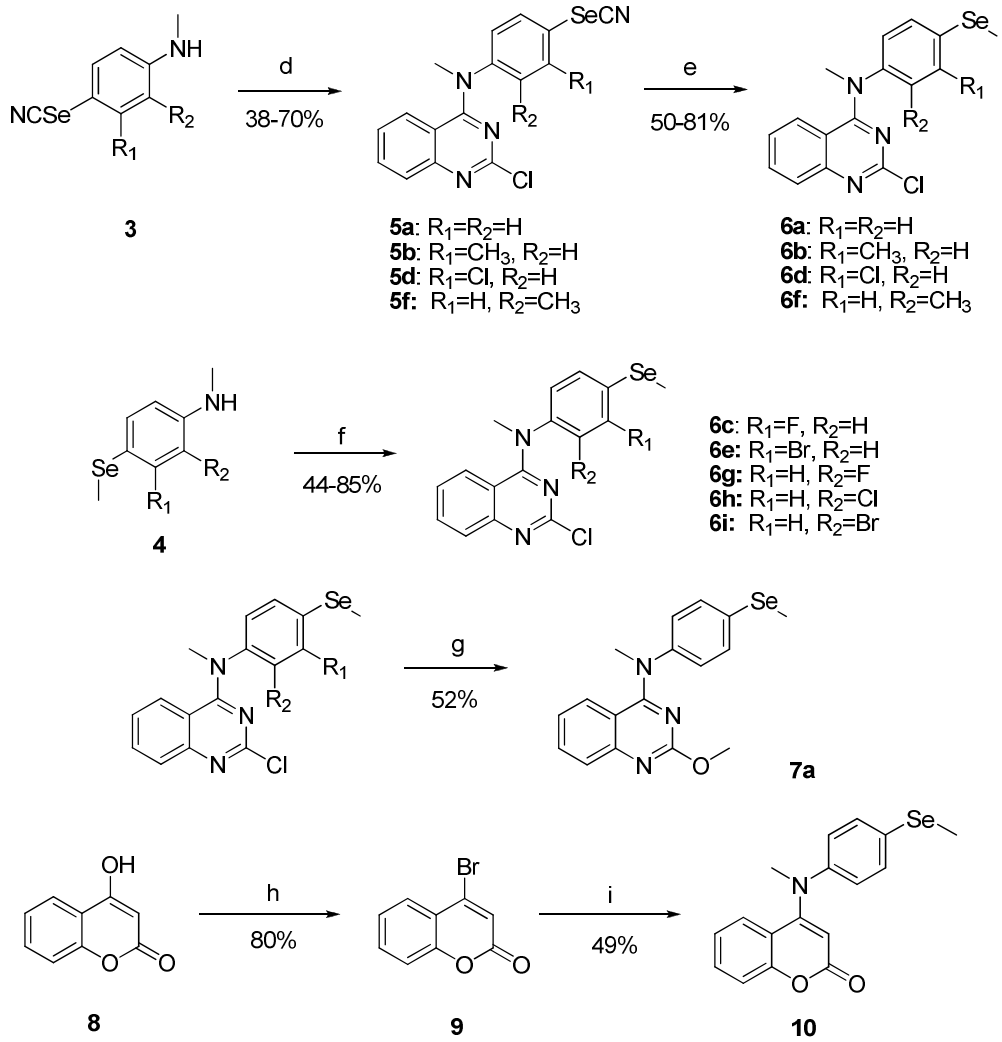

Scheme 2. The synthesis of target compounds **5**, **6**, **7a** and **10** Reagents and conditions: (d) 2, 4-dichloroquinazoline, HCl, IPA, 12h, r.t. (e) $NaBH_4$, CH_3I, CH_3OH, 5min, r.t. (f) **4c** or **4g**, 2, 4-dichloroquinazoline, NaOAc, THF/H_2O=1:1, 2h, 70°C; **4e**, **4h** or **4i**, 2,4-dichloroquinazoline, NaH,

View Article Online
DOI: 10.1039/C8OB00875B

DMF, 8h, r.t. (g) NaOH, CH_3OH, H_2O, 3h, 50°C. (h) Bu_4NBr, P_2O_5, Toluene, 1h, 120°C. (i) 2, 4-dichloroquinazoline, DIEPA, DMF, H_2O, 12h, 110°C.

In vitro human cancer cell lines growth inhibition and the SARs

To evaluate the antiproliferative activities of the selenium-containing 4-anilinoquinazoline hybrids, all the synthesized compounds were screened against a panel of six human tumor cell lines (RKO, human colon cancer cell line; HEPG2, Human hepatoma carcinoma cells; MCF-7, breast adenocarcinoma; HeLa, human epithelial cervical cancer cell line; HCT-116, human colon cancer cell line; MGC803, humaan gastric cancer cell line). The results summarized in **Table 1** indicated that all the target compounds possess excellent antiproliferative activities with the IC_{50} at the nM level. Among them, compound **5a**, 2-chloro-N-methyl-N-(4-selenocyanatophenyl)quinazolin-4-amine exhibited the best results with the IC_{50} values ranged from 2.09 to 9.98 nM against for the six human tumor cell lines. The study of the structure and activity relationship shows that the substituent R_1 and R_2 in the aniline moiety have a great influence on activity. The methyl on R_1 or R_2 position is obviously not favorable for the activity. For example, **5b**, with the methyl on 3-position, exhibited 6.01-22.7 nM of the IC_{50} values, while **5f**, with the methyl on 2-position, provided even weaker (37.9-79.4 nM). Compound series 6, with 4-methylselanyl on aniline moiety, also provided very potent activities and exhibited the similar tendency of relationship between structure and activity. However, in some case, this series gave relatively slightly weaker activities than their 4-selenocyanatophenyl analogues (comparison the activity between **5a** and **6a**; **5b** and **6b**). This result is slightly different from our previous study of N,2-dimethyl-N-phenylquinazolin-4-amine selenium-containing derivatives as anticancer agents, which the 4-methylselanyl (on aniline moiety) derivatives gave the best results. Compound **10**, selenium-coumarin derivatives, exhibited 17.4-89.5 nM of the IC_{50} values indicating that the quinazolin structure is a better pharmacophore than coumarin in these compounds.

Table 1. Anti-proliferative activities of **s**ynthesized selenium-containing 4-anilinoquinazoline derivatives against human cancer cell lines

View Article Online
DOI: 10.1039/C8OB00875B

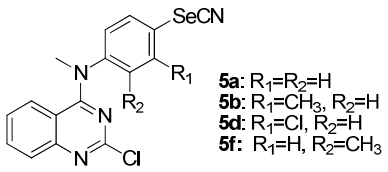

5a: R_1=R_2=H
5b: R_1=CH_3, R_2=H
5d: R_1=Cl, R_2=H
5f: R_1=H, R_2=CH_3

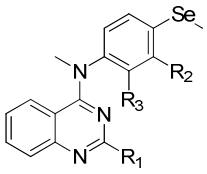

6a: R_1=Cl, R_2=R_3=H
6b: R_1=Cl, R_2=CH_3, R_3=H
6c: R_1=Cl, R_2=F, R_3=H
6d: R_1=Cl, R_2=Cl, R_3=H
6e: R_1=Cl, R_2=Br, R_3=H
6f: R_1=Cl, R_2=H, R_3=CH_3
6g: R_1=Cl, R_2=H, R_3=F
6h: R_1=Cl, R_2=H, R_3=Cl
6i: R_1=Cl, R_2=H, R_3=Br
7a: R_1=OCH_3, R_2=R_3=H

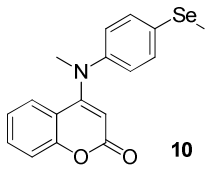

10

Comp.	IC_{50} (nM)[b]					
	RKO	HEPG2	MCF7	HELA	HCT116	MGC803
5a	3.39±0.002	5.24±0.003	9.98±0.007	2.09±0.003	4.97±0.004	3.54±0.005
5b	6.01±0.002	6.79±0.004	18.9±0.002	8.73±0.004	22.7±0.009	16.5±0.001
5d	3.42±0.002	6.78±0.003	10.6±0.009	6.78±0.005	9.17±0.006	9.67±0.004
5f	47.1±0.011	37.9±0.009	78.9±0.013	38.9±0.009	79.4±0.015	55.7±0.011
6a	4.61±0.003	6.81±0.004	14.7±0.010	2.77±0.002	8.99±0.003	5.46±0.002
6b	15.0±0.005	17.9±0.003	36.1±0.008	12.6±0.003	45.9±0.019	9.96±0.004
6d	4.55±0.001	4.79±0.004	14.3±0.011	6.93±0.001	11.7±0.004	9.93±0.002
6f	33.1±0.009	19.5±0.003	91.3±0.016	57.8±0.007	78.4±0.013	44.5±0.008
6c	7.87±0.002	13.2±0.009	22.5±0.017	9.28±0.09	12.3±0.06	14.8±0.011
6e	14.9±0.009	8.90±0.007	32.8±0.008	16.9±0.010	34.3±0.009	38.3±0.012
6g	12.9± 0.007	52.6±0.009	96.8±0.013	11.1±0.004	45.6±0.010	55.6±0.015
6h	43.5±0.011	50.8± 0.008	95.7± 0.032	29.5± 0.008	48.9±0.024	53.8±0.090
6i	76.8± 0.09	58.8± 0.012	53.5± 0.007	49.8± 0.008	63.4± 0.016	48.9± 0.007
7a	7.85±0.004	8.92±0.002	22.7±0.010	9.15±0.002	11.4±0.010	4.78±0.004
10	17.4±0.005	89.5±0.015	74.9±0.022	84.1±0.007	63.4±0.016	44.8±0.018
EP128495	4.22±0.001	6.47±0.001	5.61±0.001	5.11±0.002	8.27±0.001	6.23±0.008

[a] Cell lines were treated with compounds for 48 h. Cell viability was measured by MTT assay as described in the Experimental Section. [b] IC_{50} values are indicated as the mean ± SD (standard error) of at least three independent experiments.

Selectivity of 5a towards normal cells.

As compound **5a** exhibited excellent antiproliferative activity in the initial cytotoxicity screening, we further evaluated their activities against human normal cells (LO2, human normal liver cells; BJ, human dermal fibroblast cells; HLF, human embryonic lung fibroblast cells). It can be seen from **table 2** that **5a** exhibited no obvious cytotoxicity against human normal cells in a broad concentration range (14.5-17.2 nM) for 48 h, the selectivity factor values (RF: 7.2, 6.9 and 8.3) displayed **5a** possess less potent anti-proliferative activities towards human normal cell lines which deserve further study.

View Article Online
DOI: 10.1039/C8OB00875B

Table 3. Anti-proliferative activities of compound **5a** towards human normal cell lines

Cell lines	LO2	BJ	HLF	HELA
IC_{50} (nM)[a]	15.1±0.003	14.5±0.005	17.2±0.006	2.09±0.003
Selectivity ratio[b]	7.2	6.9	8.3	

[a] Data are presented as the mean ± SE from the dose-response cures of at least three independent experiments. [b] Selectivity ratio = (IC_{50} human normal cells) / (IC_{50} HELA).

Inhibition of tubulin polymerization *in vitro*

Cai et al. have confirmed that EP128495 could inhibit41 tubulin polymerization. To determine whether the synthesized selenium-containing compounds could target the tubulin microtubule system, we used compound **5a**, which exhibited relatively better antiproliferative activities in the initial cytotoxicity screening among all the tested compounds, for the in vitro tubulin polymerization inhibition activity assay. After the purified and unpolymerized tubulin was incubated with **5a** in the concentrations of 0.75, 1.25, 2.5, 5.0 and 10 μM, the polymerization was measured by the method of fluorescence intensity assay. As shown in **Fig. 2**, the fluorescence intensity of the control samples increased with time at 37°C indicating the tubulin polymerization had occurred. When tubulin was incubated with the **5a** at increased concentrations, the increase of the fluorescence intensity was obviously slowed down. The inhibitory concentrations that reduced the polymerized tubulin by 50% (IC_{50}) of compound **5a** was 1.88 ± 0.11 μM, being stronger than the reference compound EP128495 (IC_{50}: 2.74±0.09 μM).

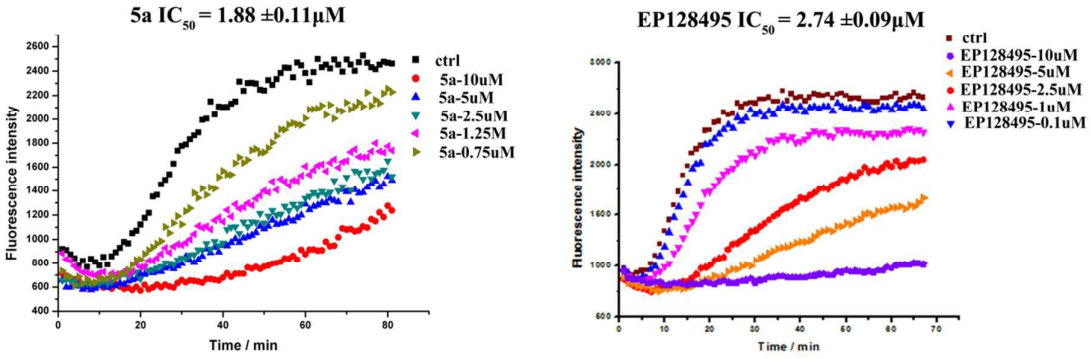

Fig.2 Effects of compounds **5a** compared to EP128495 on microtubule dynamics. Purified tubulin protein at 10 mM in a reaction buffer was incubated at 37 °C in the absence (control) or presence of **5a** at the indicated concentrations (ranging from 0.75 to 10 μM). Polymerizations are followed by an increase

View Article Online
DOI: 10.1039/C8OB00875B

in fluorescence emission at 410 nM over a 90 min period at 37 °C (excitation wavelength was 340 nM). The experiments were performed three times, and the results of representative experiments are shown.

Detection of microtubule immunofluorescence

Tubulin-microtubule systems are very important in the maintenance of cellular morphology. To reveal if compound **5a** could affect microtubule dynamics in living cells, immunofluorescence assay in human lung epithelium cancer cells (A549) and human epithelial cervical cancer (Hela) cells were performed (**Fig**. **3**). The control group was observed to be predominantly in interphase of the cell cycle, which was characterized by uncondensed chromosomes and the regularly assembled, slim, fibrous microtubules wrapped around the cell nucleus. In contrast, the microtubule network became disorganized with the treatment of compound **5a** at 1 nM of the concentration. When the concentration was increased to 5 nM, the microtubule network was completely disrupted. These morphological changes of microtubules suggest that compound **5a** effectively disrupts the microtubule dynamics, which might leads to cell death eventually.

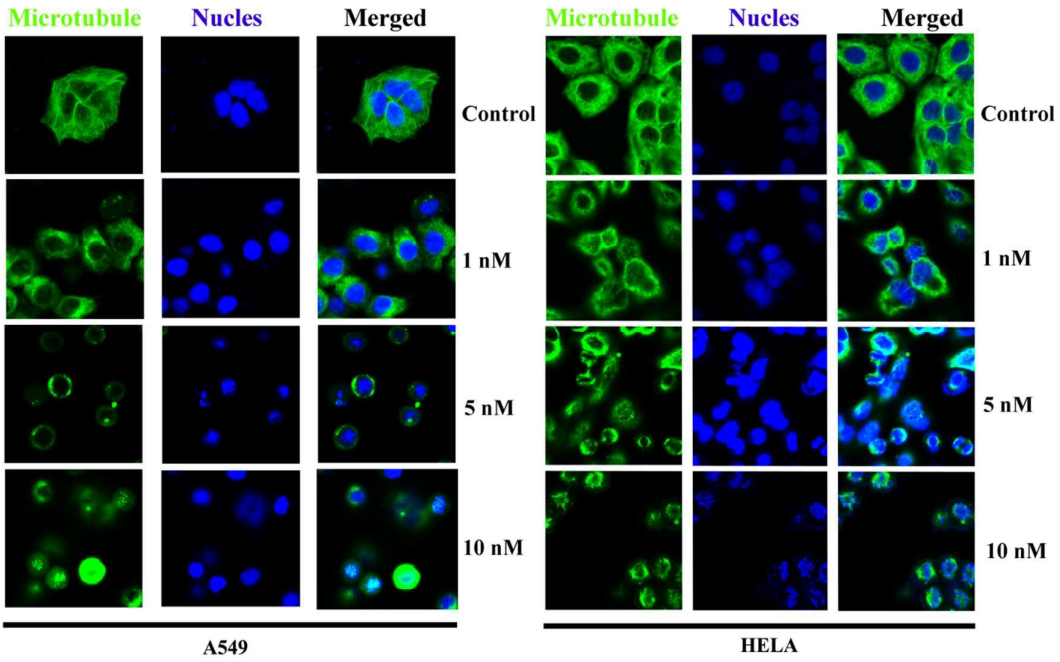

Fig.3 Effect of hybrid compounds **5a** on the microtubule network and the nucleus morphology. Cultured A549 and HeLa cells were incubated in the presence of varying concentrations of compound **5a** for 8 h.

View Article Online
DOI: 10.1039/C8OB00875B

The samples were stained for immunofluorescence using Alexa-Fluor 488 antibody (green) and corresponding Hoechst 33342 conjugated (blue). Images of the spindle microtubule were taken under LSM 570 laser confocal microscope. The results represent the best of data collected from three experiments with similar results (n = 3).

Induction of mitotic arrest

As we know, tubulin-destabilizing agents could block the cell cycle in the G2/M phase because of microtubule depolymerization and cytoskeleton disruption.[31] On the base of the in vitro tubulin polymerization inhibition activity and detection of morphological aberrations assay, we then evaluated the effects on the cell cycle progression of compound **5a** by flow cytometry method. After treatment with increasing concentrations of **5a** for 12 h or 24 h, cells were harvested, fixed with 70% ethanol, and stained with propidium iodide (PI) for the assay. The results (**Fig.4**) indicated that treatment with **5a** results a dose-dependent accumulation of HELA cells in the G2/M phase with concomitant losses in G1 phase. The changes of S phase were not observed during the entire 12 or 24 h treatments. On the other hand, sub-G phase, which indicates apoptotic cells, was obviously found as the concentration of **5a** increased, especially after the treatment for 24 hours. Altogether, the above results demonstrated that **5a** induces cell-cycle progression arrest in G2/M phase, which is in agreement with the activity of most antimitotic agents.

View Article Online
DOI: 10.1039/C8OB00875B

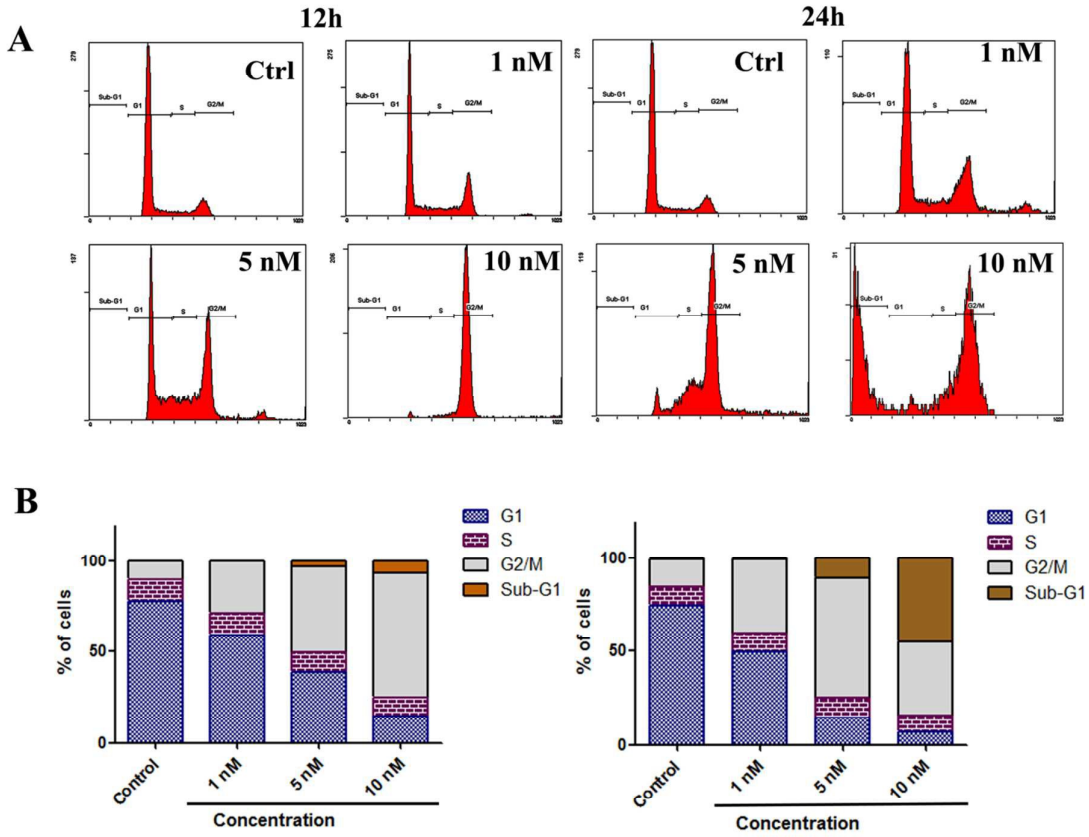

Fig. 4 Effect of **5a** on cell cycle progression. HELA cells (3×10^5 cells/sample) were treated with increasing concentrations of **5a** for 12 h or 24 h. (A) Cells were harvested, fixed with 70% ethanol, and stained with propidium iodide (PI). The cellular DNA content was then determined by flow cytometry analysis. (B) Quantitative analysis of the percentage of cells in each cell cycle phase was analyzed by EXPO32 ADC analysis software. The experiments were performed for three times, and the results of representative experiments are shown.

Induction of mitotic cell apoptosis

Cell apoptosis is a process that organisms eliminate excessive cells and control cell numbers.[32] Promoting apoptosis has been suggested as a promising strategy for cancer drug discovery.[33] To determine whether compound **5a** could induce cell apoptosis, we carried out the cell apoptosis assay. After **5a**-treated HELA cells (24 or 48 h) were stained with Annexin V-FITC and PI, the samples were analyzed by flow cytometry. As shown in **Fig. 5A**, 18.55% of the early and late apoptosis were obtained in HELA cells treated with **5a** for 24 h at 1.0 nM of the concentration. The

View Article Online
DOI: 10.1039/C8OB00875B

numbers increased to 34.55% at 5.0 nM of the concentration and arrived to 51.15% at 20 nM. After incubation for 48 h, the total percentage of early and late apoptotic cells was 24.73%, 50.30%, and 65.63% in the cases of 1, 5 and 10 nM of **5a**, respectively. In contrast, only 1.11% and 1.28% of the early and late apoptotic cells were detected in the control cells. To further determine whether **5a**-induced cell death is concerned with Bcl-2 family, we treated hela cells with **5a** for 48 h, and detected the level of proteins Bax, Bad and Bcl2. As shown in **Fig. 5C**, the proapoptotic protein increased significantly with the increase of drug concentration (e.g., Bax and Bad), and accompanied the anti-apoptotic protein Bcl-2 reduction significantly. Overall, the results above suggest that **5a** could efficiently induced cell apoptosis in a dose-dependent and time-dependent manner.

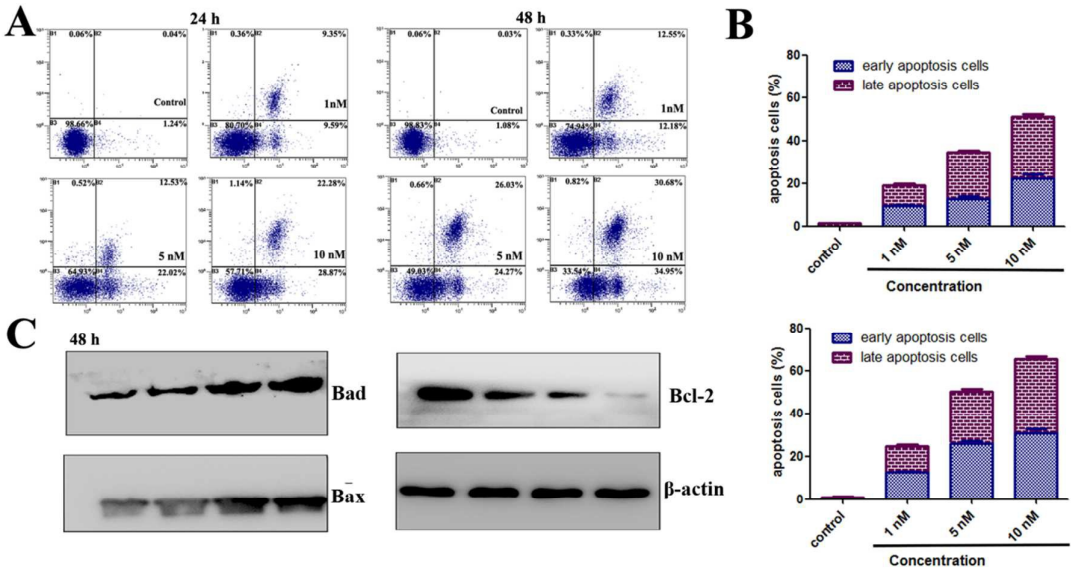

Fig. 5 Inhibition of proliferation and induction of apoptosis in HELA cells treated with **5a**. (A) Treated with **5a** (1, 5 and 10 nM) for 24 h or 48h. (B) Total apoptosis cells percentage (obtained by EXPO32 ADC analysis software). (C) The expression of proteins (Bax, Bad and Bcl2) by the western blot assay. The experiments were performed for three times.

Loss of Mitochondrial Potential and ROS Generation

Studies have shown that progression of apoptosis is closely related to mitochondria.[34] It is thought a signal of apoptosis to be the decreased mitochondrial membrane potential (MMP, $\Delta\Psi$ m). To evaluate whether the target compounds were associated with apoptosis, we used flow cytometry analysis and a laser scanning confocal microscope to detect the MMP. **Fig.**

View Article Online
DOI: 10.1039/C8OB00875B

6A showed that after cells exposed to **5a** at the concentration of 1.0 nM, the red fluorescence intensity (JC-1 aggregates) decreased from 98.28% (control) to 91.88%; correspondingly, the green fluorescence intensity (JC-1 monomers) increase from 1.72% to 8.12%. When the concentration of **5a** increased from 5.0 to 10 nM, JC-1 monomers increased from 31.12% to 71.48%, which also showed a dose-dependent manner. **Fig. 6B** exhibited the results of confocal microscopy. With the concentration of **5a** increased, there is a shift from aggregates (red fluorescence) toward the form of the monomers (green fluorescence), which is consistent with the results of the flow cytometry analysis, and demonstrated that compound **5a** lead to mitochondrial dysfunction.

Reactive oxygen species (ROS) are closely related to tumorigenesis and the apoptosis of cancer cells through DNA damage in the cell nucleus.[35] In cancer cells, growth and proliferation are encouraged with a condition of a modest rise in intracellular ROS, and on the other hand, apoptosis is also induced by a higher levels of ROS. To determine whether compound **5a** could induce ROS accumulation, the laser scanning confocal microscope assay was performed to evaluate the generation of intracellular ROS in Hela cells. The green fluorescence in **Fig 6D**, which reflects the level of intracellular ROS, was more and more to observe after compound **5a** was added to the cells at the concentration from 1.0 to 10 nM for 12 h. In contrast, green fluorescence was difficulty to be observed in the control. **Fig. 6C** indicated the results of quantitative analysis, which also showed that compound **5a** induced mitochondrial depolarization and thus resulted in the intracellular ROS production.

View Article Online
DOI: 10.1039/C8OB00875B

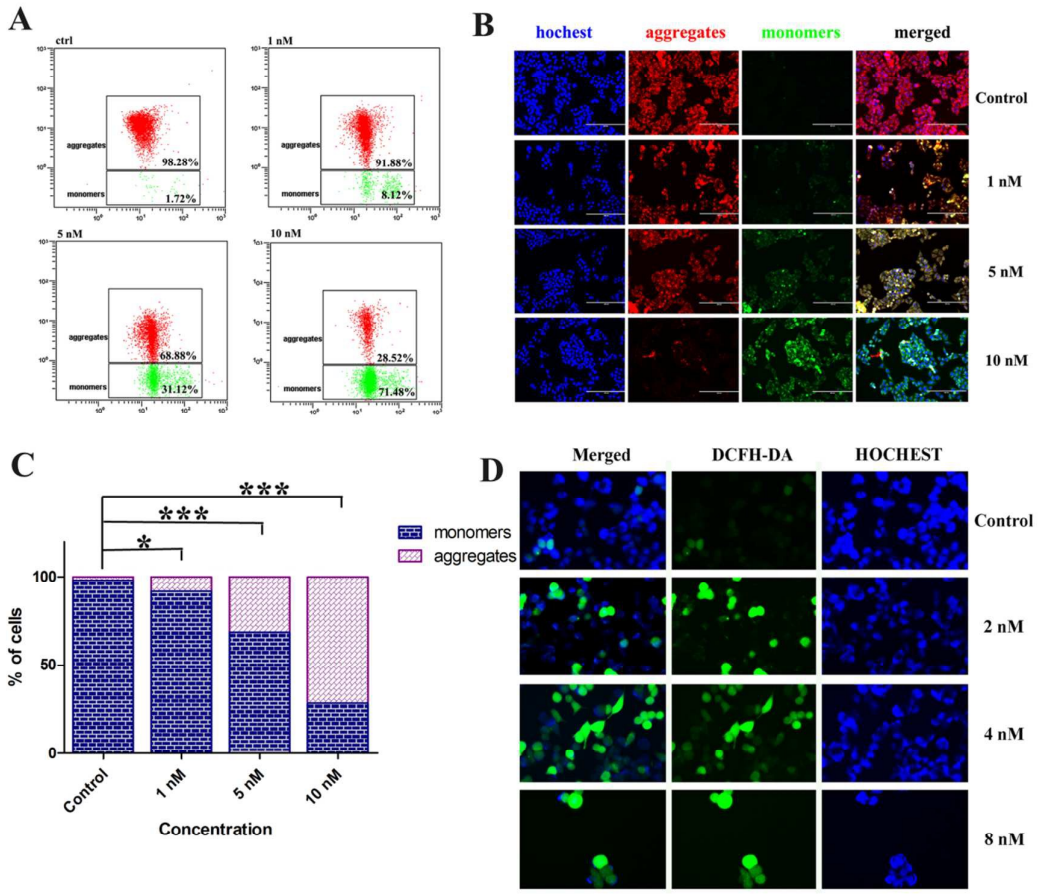

Fig. 6 Decreased the mitochondrial membrane potential and increased ROS levels by **5a** of Hela cells. The Hela cells were treated with **5a** at different concentrations (1, 5, and 10 nM) or DMSO (0.01%) for 24 h, followed by incubation with the fluorescent probe JC-1 for 30 min. Then, the cells were analyzed by flow cytometry (A) or fluorescence microscopy (B). (D)The fluorescence images demonstrate the motivation of **5a**-induced ROS. The experiments were performed at least three times, and the results of the representative experiments are shown. *P<0.05, ***P<0.001 vs. the control group.

Conclusions

We have developed a series of new selenium-containing 4-anilinoquinazoline derivatives by inducing the selenium the molecular, which the element is an essential trace mineral nutrient with multiple roles in human health, to obtain a series of new tubulin

View Article Online
DOI: 10.1039/C8OB00875B

polymerization inhibitors. The cytotoxic activities of all these compounds and the interactions of some of them with tubulin have been investigated. Among them, compound **5a**, (2-chloro-N-(4-methoxyphenyl)-N-methylquinazolin-4-amine), possessed potent antiproliferative abilities,with IC_{50} values ranging from 3.39 to 9.98 nM against all the tested tumor cell lines. Preliminary mode of action studies demonstrated that **5a** arrested most cells in the G2/M phase of the cell and disrupted cellular microtubules and induced apoptosis in HELA cells. In addition, mechanism considerations suggested that the induction of apoptosis was related to loss of mitochondrial potential and ROS generation. In a summary, these newly developed compounds showed marked biological activity and have potential for further development as a novel class of anticancer agents.

Experimental

Unless otherwise noted, all commercially available solvents and reagents were analytically pure used without further purification. ^{1}H NMR and ^{13}C NMR were recorded on a Bruker Avance 400 spectrometer (Bruker Company, Germany) in $CDCl_3$ using TMS as an internal standard. Chemical shifts are quoted in ppm (parts per million). High-resolution mass spectra (HRMS) were determined using a Shimadzu LCMS-ITTOF mass spectrometer. Melting points (MP) of all the final solid compounds were determined on SRS-OptiMelt automated melting point instrument. The purity of all the final synthesized compounds screened in biological assays were determined to be >95% by HPLC analysis with an Agilent LC–MS 6120 instrument (column, Eclipse Plus C8 column 4.6 × 150 mm, 5 μm; mobile phase, acetonitrile(90%)/ water (10%); flow rate, 0.20 mL/min, injection volume, 2 μL; UV wavelength, 214−400 nm).

General procedure for the preparation of 2a-2i

Sodium (2.3 g, 100 mmol) was dissolved in methanol (200 mL) at 0 . Paraformaldehyde (0.84g, 28 mmol) was added to the above solution and then stirred overnight at room temperature. Substituted phenylamine **1** (20 mmol) was added and then $NaBH_4$ (0.76g, 20.0

View Article Online
DOI: 10.1039/C8OB00875B

mmol). After the reaction was constituted at 60□ for 2-4 hours, the solvent was evaporated, and water was added. The mixture was extracted with ethyl acetate and then washed (brine), dried (Na_2SO_4). Evaporation of the solvents to afford the crude product which was purified by silica gel chromatography (petroleum ether: ethyl acetate=20:1) to yield the intermediate compounds **2a-2i**.

N-methylaniline (2a)

Colorless oil, yield: 85%. ^{1}H NMR (400 MHz, $CDCl_3$) δ 7.16 (dd, *J* = 8.5, 7.4 Hz, 2H), 6.68 (t, *J* = 7.8 Hz, 1H), 6.55 (dd, *J* = 8.6, 0.9 Hz, 2H), 3.57 (s, 1H), 2.73 (s, 3H). ^{13}C NMR (101 MHz, $CDCl_3$) δ 149.55 (s), 129.36 (s), 117.34 (s), 112.58 (s), 30.82 (s).

N,3-dimethylaniline (2b)

Colorless oil, yield: 82%. ^{1}H NMR (400 MHz, $CDCl_3$) δ 6.99 (t, *J* = 8.1 Hz, 1H), 6.45 (d, *J* = 7.3 Hz, 1H), 6.34 (d, *J* = 6.4 Hz, 2H), 3.40 (s, 1H), 2.72 (s, 3H), 2.20 (s, 3H). ^{13}C NMR (101 MHz, $CDCl_3$) δ 149.48 (s), 139.01 (s), 129.13 (s), 118.26 (s), 113.25 (s), 109.70 (s), 30.82 (s), 21.69 (s).

3-fluoro-N-methylaniline (2c)

Colorless oil, yield: 70%. ^{1}H NMR (400 MHz, $CDCl_3$) δ 7.07 (dd, *J* = 14.9, 8.1 Hz, 1H), 6.35 (ddd, *J* = 10.1, 8.5, 2.6 Hz, 2H), 6.26 (dt, *J* = 11.7, 2.3 Hz, 1H), 3.75 (s, 1H), 2.77 (s, 3H). ^{13}C NMR (101 MHz, $CDCl_3$) δ 164.27 (d, *J* = 242.3 Hz), 151.22 (d, *J* = 10.7 Hz), 130.24 (d, *J* = 10.3 Hz), 108.39 (d, *J* = 2.2 Hz), 103.51 (d, *J* = 21.6 Hz), 98.92 (d, *J* = 25.3 Hz), 30.57 (s).

3-chloro-N-methylaniline (2d)

Colorless oil, yield: 82%. ^{1}H NMR (400 MHz, $CDCl_3$) δ 7.05 (t, *J* = 8.0 Hz, 1H), 6.64 (d, *J* = 7.8 Hz, 1H), 6.53 (s, 1H), 6.42 (dd, *J* = 8.1, 1.6 Hz, 1H), 3.73 (s, 1H), 2.75 (s, 3H). ^{13}C NMR (101 MHz, $CDCl_3$) δ 150.53 (s), 135.05 (s), 130.20 (s), 116.99 (s), 111.92 (s), 110.89 (s), 30.55 (s).

View Article Online
DOI: 10.1039/C8OB00875B

3-bromo-N-methylaniline (2e)

Colorless oil, yield: 93%. ^{1}H NMR (400 MHz, $CDCl_3$) δ 6.98 (t, J = 8.0 Hz, 1H), 6.78 (d, J = 7.8 Hz, 1H), 6.68 (s, 1H), 6.45 (dd, J = 8.2, 2.2 Hz, 1H), 3.71 (s, 1H), 2.73 (s, 3H). ^{13}C NMR (101 MHz, $CDCl_3$) δ 150.67 (s), 130.52 (s), 123.34 (s), 119.87 (s), 114.82 (s), 111.30 (s), 30.56 (s).

N,2-dimethylaniline (2f)

Colorless oil, yield: 83%. ^{1}H NMR (400 MHz, $CDCl_3$) δ 7.08 (t, J = 7.7 Hz, 1H), 6.97 (d, J = 7.2 Hz, 1H), 6.59 (t, J = 7.3 Hz, 1H), 6.53 (d, J = 8.0 Hz, 1H), 3.46 (s, 1H), 2.80 (s, 3H), 2.05 (s, 3H). ^{13}C NMR (101 MHz, $CDCl_3$) δ 146.20 (s), 128.86 (s), 126.15 (s), 120.86 (s), 115.81 (s), 108.09 (s), 29.73 (s), 16.35 (s).

2-fluoro-N-methylaniline (2g)

Colorless oil, yield: 65%. ^{1}H NMR (400 MHz, $CDCl_3$) δ 6.94 (t, J = 7.7 Hz, 1H), 6.87 (dd, J = 11.9, 8.0 Hz, 1H), 6.60 (t, J = 8.4 Hz, 1H), 6.57 – 6.50 (m, 1H), 3.84 (s, 1H), 2.78 (s, 3H). ^{13}C NMR (101 MHz, $CDCl_3$) δ 151.65 (d, J = 238.3 Hz), 137.84 (d, J = 11.5 Hz), 124.64 (d, J = 3.5 Hz), 116.39 (d, J = 6.9 Hz), 114.19 (d, J = 18.2 Hz), 111.53 (d, J = 3.4 Hz), 30.25 (s).

2-chloro-N-methylaniline (2h)

Colorless oil, yield: 84%. ^{1}H NMR (400 MHz, $CDCl_3$) δ 7.17 (d, J = 7.1 Hz, 1H), 7.09 (t, J = 7.7 Hz, 1H), 6.56 (t, J = 8.3 Hz, 2H), 4.26 (s, 1H), 2.82 (d, J = 5.0 Hz, 3H). ^{13}C NMR (101 MHz, $CDCl_3$) δ 145.03 (s), 128.98 (s), 127.86 (s), 119.07 (s), 117.03 (s), 110.64 (s), 30.41 (s).

2-bromo-N-methylaniline (2i)

Colorless oil, yield: 77%. ^{1}H NMR (400 MHz, $CDCl_3$) δ 7.36 (dd, J = 7.8, 1.4 Hz, 1H),

View Article Online
DOI: 10.1039/C8OB00875B

7.19 – 7.09 (m, 1H), 6.56 – 6.46 (m, 2H), 4.26 (s, 1H), 2.74 (d, J = 5.2 Hz, 3H). ^{13}C NMR (101 MHz, $CDCl_3$) δ 146.13 (s), 132.43 (s), 128.77 (s), 117.75 (s), 110.92 (s), 109.77 (s), 30.69 (s).

General procedure for the preparation of 3a-3i

SeO_2 (1.33 g, 12 mmol) was added to the solution of malononitrile (396 mg, 6 mmol) in DMSO. After the mixture was stirred at room temperature for 1 hours, compounds **2** (10 mmol) was added, and the reaction was stirred for 4 hours until conversion was completed. Water was added to the mixture and then ethyl acetate. The organic phase was separated, washed (brine), dried (Na_2SO_4) and evaporated to afford crude product **3**, which was purified by silica gel chromatography (petroleum ether: ethyl acetate=10:1).

N-methyl-4-selenocyanatoaniline (3a)

White soild, yield: 75%. ^{1}H NMR (400 MHz, $CDCl_3$) δ 7.45 (d, J = 8.8 Hz, 2H), 6.54 (d, J = 8.8 Hz, 2H), 4.10 (s, 1H), 2.82 (d, J = 4.3 Hz, 3H). ^{13}C NMR (101 MHz, $CDCl_3$) δ 151.11 (s), 136.63 (s), 113.55 (s), 105.18 (s), 102.99 (s), 30.23 (s).

N,3-dimethyl-4-selenocyanatoaniline (3b)

White soild, yield: 70%. ^{1}H NMR (400 MHz, $CDCl_3$) δ 7.47 (d, J = 8.5 Hz, 1H), 6.51 (d, J = 2.5 Hz, 1H), 6.37 (dd, J = 8.5, 2.7 Hz, 1H), 4.00 (s, 1H), 2.82 (s, 3H), 2.49 (s, 3H). ^{13}C NMR (101 MHz, $CDCl_3$) δ 151.71 (s), 143.27 (s), 137.90 (s), 114.39 (s), 111.13 (s), 107.05 (s), 102.49 (s), 30.24 (s), 23.36 (s).

3-fluoro-N-methyl-4-selenocyanatoaniline (3c)

White soild, yield: 82%. ^{1}H NMR (400 MHz, $CDCl_3$) δ 7.41 (t, J = 7.8 Hz, 1H), 6.35 (d, J = 9.4 Hz, 2H), 4.25 (s, 1H), 2.84 (d, J = 5.1 Hz, 3H). ^{13}C NMR (101 MHz, $CDCl_3$) δ 163.29 (d, J = 245.8 Hz), 153.83 (d, J = 10.9 Hz), 137.36 (d, J = 2.6 Hz), 109.90 (d, J = 2.1 Hz), 101.55 (s), 99.13 (d, J = 26.8 Hz), 91.65 (d, J = 22.5 Hz), 30.22 (s).

View Article Online
DOI: 10.1039/C8OB00875B

3-chloro-N-methyl-4-selenocyanatoaniline (3d)

White soild, yield: 79%. ^{1}H NMR (400 MHz, $CDCl_3$) δ 7.49 (d, *J* = 8.7 Hz, 1H), 6.66 (d, *J* = 2.6 Hz, 1H), 6.47 (dd, *J* = 8.7, 2.6 Hz, 1H), 4.14 (s, 1H), 2.83 (d, *J* = 5.1 Hz, 3H). ^{13}C NMR (101 MHz, $CDCl_3$) δ 151.84 (s), 137.52 (s), 135.69 (s), 112.88 (s), 112.63 (s), 106.07 (s), 101.92 (s), 30.24 (s).

3-bromo-N-methyl-4-selenocyanatoaniline (3e)

White soild, yield: 87%. ^{1}H NMR (400 MHz, $CDCl_3$) δ 7.50 (d, *J* = 8.7 Hz, 1H), 6.82 (d, *J* = 2.6 Hz, 1H), 6.52 (dd, *J* = 8.7, 2.6 Hz, 1H), 4.10 (s, 1H), 2.82 (d, *J* = 5.2 Hz, 3H). ^{13}C NMR (101 MHz, $CDCl_3$) δ 151.54 (s), 135.09 (s), 127.11 (s), 116.08 (s), 113.28 (s), 108.78 (s), 102.42 (s), 30.26 (s).

N,2-dimethyl-4-selenocyanatoaniline (3f)

White soild, yield: 77%. ^{1}H NMR (400 MHz, $CDCl_3$) δ 7.43 (dd, *J* = 8.4, 1.9 Hz, 1H), 7.34 (s, 1H), 6.52 (d, *J* = 8.5 Hz, 1H), 3.89 (s, 1H), 2.89 (d, *J* = 4.8 Hz, 3H), 2.09 (s, 3H). ^{13}C NMR (101 MHz, $CDCl_3$) δ 149.16 (s), 136.47 (s), 134.75 (s), 123.72 (s), 110.07 (s), 104.85 (s), 103.05 (s), 30.41 (s), 17.17 (s).

2-fluoro-N-methyl-4-selenocyanatoaniline (3g)

White soild, yield: 74%. ^{1}H NMR (400 MHz, $CDCl_3$) δ 7.32 (d, *J* = 8.5 Hz, 1H), 7.27 (d, *J* = 10.6 Hz, 1H), 6.60 (t, *J* = 8.6 Hz, 1H), 4.30 (s, 1H), 2.86 (d, *J* = 5.2 Hz, 3H). ^{13}C NMR (101 MHz, $CDCl_3$) δ 150.89 (d, *J* = 244.9 Hz), 140.11 (d, *J* = 11.4 Hz), 132.47 (d, *J* = 3.1 Hz), 120.75 (d, *J* = 20.0 Hz), 111.96 (d, *J* = 3.9 Hz), 103.67 (d, *J* = 7.1 Hz), 102.38 (s), 29.75 (s).

2-chloro-N-methyl-4-selenocyanatoaniline (3h)

White soild, yield: 82%. ^{1}H NMR (400 MHz, $CDCl_3$) δ 7.57 (d, *J* = 2.1 Hz, 1H), 7.46 (dd,

View Article Online
DOI: 10.1039/C8OB00875B

J = 8.5, 2.0 Hz, 1H), 6.59 (d, *J* = 8.6 Hz, 1H), 4.68 (s, 1H), 2.91 (d, *J* = 5.1 Hz, 3H). ^{13}C NMR (101 MHz, $CDCl_3$) δ 146.84 (s), 135.32 (s), 135.30 (s), 119.63 (s), 111.37 (s), 104.68 (s), 102.28 (s), 30.10 (s).

2-bromo-N-methyl-4-selenocyanatoaniline (3i)

White soild, yield: 75%. ^{1}H NMR (400 MHz, $CDCl_3$) δ 7.73 (d, *J* = 2.1 Hz, 1H), 7.50 (dd, *J* = 8.6, 2.0 Hz, 1H), 6.57 (d, *J* = 8.6 Hz, 1H), 4.69 (s, 1H), 2.91 (d, *J* = 5.1 Hz, 3H). ^{13}C NMR (101 MHz, $CDCl_3$) δ 147.74 (s), 138.47 (s), 135.90 (s), 111.41 (s), 109.79 (s), 105.21 (s), 102.27 (s), 30.34 (s).

General procedure for the preparation of 5a, 5b, 5d, 5f

To a solution containing **3** (**3a**, **3b**, **3d**, **3f**, 1 mmol, respectively) and 2, 4-dichloroquinazoline (199 mg, 1 mmol) in 30 mL IPA, HCl (12N, 0.5 mL) was added. The mixture was stirred for 5-8 hours and then filtered. The precipitate was purified by silica gel chromatography with petroleum ether/ethyl acetate (5: 1) to get the title compounds **5a**, **5b**, **5d** and **5f**.

2-chloro-N-methyl-N-(4-selenocyanatophenyl)quinazolin-4-amine (5a)

White soild, yield: 70%. mp: 142.2°C -143.2°C. ^{1}H NMR (400 MHz, $CDCl_3$) δ 7.79 (dd, *J* = 8.3, 3.7 Hz, 1H), 7.66 (dd, *J* = 8.5, 1.9 Hz, 2H), 7.62 (dd, *J* = 8.4, 1.7 Hz, 1H), 7.22 (d, *J* = 1.7 Hz, 1H), 7.20 (s, 1H), 7.14 – 7.08 (m, 1H), 6.99 (dd, *J* = 8.5, 1.4 Hz, 1H), 3.66 (d, *J* = 3.0 Hz, 3H). ^{13}C NMR (101 MHz, $CDCl_3$) δ 163.11 (s), 156.54 (s), 153.17 (s), 149.19 (s), 134.70 (s), 133.29 (s), 128.11 (s), 127.35 (s), 126.02 (s), 125.75 (s), 119.45 (s), 114.83 (s), 101.01 (s), 42.66 (s). ESI-MS (*m/z*) 375.0 $[M+H]^+$; (HRMS (ESI) (*m/z*) $[M+Na]^+$ calcd for $C_{16}H_{11}ClN_4Se$, 396.9728; found, 396.9726. Purity: 96.2% (by HPLC).

2-chloro-N-methyl-N-(3-methyl-4-selenocyanatophenyl)quinazolin-4-amine (5b)

White soild, yield: 39%. mp: 164.7°C -165.4°C. ^{1}H NMR (400 MHz, $CDCl_3$) δ 7.77 (dd, *J* = 21.0, 8.3 Hz, 2H), 7.61 (s, 1H), 7.15 (s, 1H), 7.11 (d, *J* = 7.2 Hz, 1H), 7.02 (d, *J* = 8.9 Hz,

View Article Online
DOI: 10.1039/C8OB00875B

2H), 3.62 (s, 3H), 2.46 (s, 3H). ^{13}C NMR (101 MHz, $CDCl_3$) δ 162.98 (s), 156.50 (s), 153.09 (s), 149.50 (s), 142.42 (s), 135.85 (s), 133.22 (s), 128.06 (s), 128.01 (s), 126.09 (s), 125.66 (s), 124.90 (s), 120.91 (s), 114.86 (s), 100.72 (s), 42.73 (s), 22.59 (s). ESI-MS (*m/z*) 389.0 $[M+H]^+$; HRMS (ESI) (*m/z*) $[M+H]^+$ calcd for $C_{17}H_{13}ClN_4Se$, 389.0065; found, 389.0063. Purity: 97.9% (by HPLC).

2-chloro-N-(3-chloro-4-selenocyanatophenyl)-N-methylquinazolin-4-amine (5d)

White soild, yield: 44%. mp: 207.7°C -208.6°C. ^{1}H NMR (400 MHz, $CDCl_3$) δ 7.83 (d, *J* = 8.2 Hz, 1H), 7.76 (d, *J* = 8.5 Hz, 1H), 7.68 (t, *J* = 7.4 Hz, 1H), 7.27 (s, 1H), 7.23 – 7.17 (m, 1H), 7.15 (d, *J* = 8.4 Hz, 1H), 7.08 (d, *J* = 8.4 Hz, 1H), 3.67 (s, 3H). ^{13}C NMR (101 MHz, $CDCl_3$) δ 163.02 (s), 156.51 (s), 153.28 (s), 149.36 (s), 134.04 (s), 133.51 (s), 132.42 (s), 128.30 (s), 126.53 (s), 126.06 (s), 125.80 (s), 125.74 (s), 121.66 (s), 114.83 (s), 100.44 (s), 42.65 (s). ESI-MS (*m/z*) 409.0 $[M+H]^+$; HRMS (ESI) (*m/z*) $[M+Na]^+$ calcd for $C_{16}H_{10}Cl_2N_4Se$, 430.9336; found, 430.9333. Purity: 95.6% (by HPLC).

2-chloro-N-methyl-N-(2-methyl-4-selenocyanatophenyl)quinazolin-4-amine (5f)

White soild, yield: 38%. mp: 153.8°C -154.3°C. ^{1}H NMR (400 MHz, $CDCl_3$) δ 7.77 (d, *J* = 7.3 Hz, 1H), 7.65 (s, 1H), 7.61 (t, *J* = 7.5 Hz, 1H), 7.53 (d, *J* = 7.9 Hz, 1H), 7.19 (d, *J* = 8.2 Hz, 1H), 7.05 (t, *J* = 7.6 Hz, 1H), 6.75 (d, *J* = 8.5 Hz, 1H), 3.54 (s, 3H), 2.22 (s, 3H). ^{13}C NMR (101 MHz, $CDCl_3$) δ 162.15 (s), 156.58 (s), 152.93 (s), 147.16 (s), 137.87 (s), 135.99 (s), 133.08 (s), 132.08 (s), 129.47 (s), 128.08 (s), 125.76 (s), 124.64 (s), 121.65 (s), 114.60 (s), 100.96 (s), 41.76 (s), 17.93 (s). ESI-MS (*m/z*) 389.0 $[M+H]^+$; HRMS (ESI) (*m/z*) $[M+Na]^+$ calcd for $C_{17}H_{13}ClN_4Se$, 410.9884; found, 410.9890. Purity: 96.4% (by HPLC).

General procedure for the preparation of 4a, 4c, 4e, 4g, 4h, 4i, 6a, 6b, 6d, 6f

To a solution of **3** (**3a**, **3c**, **3e**, **3g**, **3h**, **3i**, 10 mmol, respectively) or **5** (**5a**, **5b**, **5d**, **5f**, 10 mmol, respectively) in CH_3OH (10 mL), $NaBH_4$ (380 mg, 10 mmol) and CH_3I (920 μL, 15 mmol) were added in sequence. After the mixture was stirred at room temperature for 2 minutes, saturated $NaHSO_4$ solution was added and then ethyl acetate. The organic layer was separated, washed (brine), and dried (Na_2SO_4). Evaporation of the solvents to afford

View Article Online
DOI: 10.1039/C8OB00875B

the crude product which was purified by silica gel chromatography (petroleum ether/ethyl acetate, 5: 1) to obtain the title compounds **4a**, **4c**, **4e**, **4g**, **4h**, **4i**, **6a**, **6b**, **6d** and **6f**.

N-methyl-4-(methylselanyl)aniline (4a)

Colorless oil, yield: 75%. ^{1}H NMR (400 MHz, $CDCl_3$) δ 7.28 (d, J = 8.7 Hz, 2H), 6.45 (d, J = 8.6 Hz, 2H), 3.66 (s, 1H), 2.74 (s, 3H), 2.19 (s, 3H). ^{13}C NMR (101 MHz, $CDCl_3$) δ 148.67 (s), 134.31 (s), 116.87 (s), 113.16 (s), 30.66 (s), 9.34 (s).

3-fluoro-N-methyl-4-(methylselanyl)aniline (4c)

Colorless oil, yield: 66%. ^{1}H NMR (400 MHz, $CDCl_3$) δ 7.27 (t, J = 8.2 Hz, 1H), 6.31 (s, 1H), 6.28 (s, 1H), 3.90 (s, 1H), 2.79 (d, J = 3.7 Hz, 3H), 2.23 (s, 3H). ^{13}C NMR (101 MHz, $CDCl_3$) δ 163.55 (d, J = 240.4 Hz), 151.20 (d, J = 10.7 Hz), 135.82 (d, J = 4.7 Hz), 109.13 (d, J = 2.4 Hz), 102.33 (d, J = 23.3 Hz), 99.16 (d, J = 28.1 Hz), 30.53 (s), 8.35 (d, J = 2.1 Hz).

3-bromo-N-methyl-4-(methylselanyl)aniline (4e)

Colorless oil, yield: 79%. ^{1}H NMR (400 MHz, $CDCl_3$) δ 7.18 (d, J = 8.5 Hz, 1H), 6.79 (d, J = 2.5 Hz, 1H), 6.46 (dd, J = 8.5, 2.6 Hz, 1H), 3.76 (s, 1H), 2.76 (s, 3H), 2.26 (s, 3H). ^{13}C NMR (101 MHz, $CDCl_3$) δ 149.30 (s), 132.87 (s), 127.63 (s), 118.80 (s), 116.13 (s), 112.72 (s), 30.60 (s), 8.47 (s).

2-fluoro-N-methyl-4-(methylselanyl)aniline (4g)

Colorless oil, yield: 72%. ^{1}H NMR (400 MHz, $CDCl_3$) δ 7.09 (d, J = 8.2 Hz, 1H), 7.05 (dd, J = 11.4, 1.8 Hz, 1H), 6.49 (t, J = 8.6 Hz, 1H), 3.87 (s, 1H), 2.76 (s, 3H), 2.19 (s, 3H). ^{13}C NMR (101 MHz, $CDCl_3$) δ 150.15 (d, J = 242.3 Hz), 136.05 (d, J = 11.7 Hz), 128.30 (d, J = 3.2 Hz), 117.71 (d, J = 18.8 Hz), 114.97 (d, J = 6.0 Hz), 110.87 (d, J = 3.8 Hz), 29.12 (s), 8.17 (s).

View Article Online
DOI: 10.1039/C8OB00875B

2-chloro-N-methyl-4-(methylselanyl)aniline (4h)

Colorless oil, yield: 74%. ^{1}H NMR (400 MHz, $CDCl_3$) δ 7.41 (d, *J* = 2.0 Hz, 1H), 7.30 (dd, *J* = 8.4, 1.9 Hz, 1H), 6.52 (d, *J* = 8.4 Hz, 1H), 4.34 (s, 1H), 2.85 (d, *J* = 5.1 Hz, 3H), 2.25 (s, 3H). ^{13}C NMR (101 MHz, $CDCl_3$) δ 144.31 (s), 133.32 (s), 132.89 (s), 119.21 (s), 116.59 (s), 111.17 (s), 30.39 (s), 9.50 (s).

2-bromo-N-methyl-4-(methylselanyl)aniline (4i)

Colorless oil, yield: 80%. ^{1}H NMR (400 MHz, $CDCl_3$) δ 7.51 (d, *J* = 1.9 Hz, 1H), 7.27 (dd, *J* = 8.4, 1.8 Hz, 1H), 6.43 (d, *J* = 8.4 Hz, 1H), 4.28 (s, 1H), 2.78 (d, *J* = 5.2 Hz, 3H), 2.18 (s, 3H). ^{13}C NMR (101 MHz, $CDCl_3$) δ 145.24 (s), 136.47 (d, *J* = 4.9 Hz), 133.58 (d, *J* = 4.9 Hz), 117.12 (s), 111.22 (s), 109.66 (s), 30.59 (s), 9.60 (s).

2-chloro-N-methyl-N-(4-(methylselanyl)phenyl)quinazolin-4-amine (6a)

Green soild, yield: 68%. mp: 123.9°C -124.6°C. ^{1}H NMR (400 MHz, $CDCl_3$) δ 7.74 (d, *J* = 8.3 Hz, 1H), 7.62 – 7.52 (m, 1H), 7.43 (d, *J* = 8.5 Hz, 2H), 7.10 (d, *J* = 8.5 Hz, 2H), 7.07 – 7.01 (m, 1H), 6.98 (d, *J* = 9.3 Hz, 1H), 3.62 (s, 3H), 2.39 (s, 3H). ^{13}C NMR (101 MHz, $CDCl_3$) δ 162.72 (s), 156.57 (s), 153.02 (s), 145.32 (s), 132.81 (s), 131.58 (s), 131.26 (s), 127.78 (s), 126.66 (s), 126.35 (s), 125.21 (s), 114.81 (s), 42.95 (s), 7.29 (s). ESI-MS (*m/z*) 364.0 $[M+H]^+$; HRMS (ESI) (*m/z*) $[M+H]^+$ calcd for $C_{16}H_{14}ClN_3Se$, 364.0112; found, 364.0115. Purity: 99.3% (by HPLC).

2-chloro-N-methyl-N-(3-methyl-4-(methylselanyl)phenyl)quinazolin-4-amine (6b)

White soild, yield: 81%. mp: 164.3°C -165.3°C. ^{1}H NMR (400 MHz, $CDCl_3$) δ 7.74 (d, *J* = 8.3 Hz, 1H), 7.62 – 7.53 (m, 1H), 7.28 (d, *J* = 8.3 Hz, 1H), 7.06 – 7.01 (m, 2H), 7.00 (d, *J* = 1.1 Hz, 1H), 6.97 (dd, *J* = 8.4, 2.3 Hz, 1H), 3.61 (s, 3H), 2.36 (s, 3H), 2.34 (s, 3H). ^{13}C NMR (101 MHz, $CDCl_3$) δ 162.65 (s), 156.61 (s), 152.99 (s), 144.92 (s), 139.81 (s), 132.75 (s), 132.40 (s), 129.44 (s), 127.72 (s), 127.18 (s), 126.45 (s), 125.13 (s), 124.15 (s), 114.91 (s), 43.07 (s), 21.74 (s), 6.40 (s). ESI-MS (*m/z*) 378.0 $[M+H]^+$; HRMS (ESI) (*m/z*) $[M+H]^+$ calcd for $C_{17}H_{16}ClN_3Se$, 378.0269; found, 378.0269. Purity: 98.8% (by HPLC).

View Article Online
DOI: 10.1039/C8OB00875B

2-chloro-N-(3-chloro-4-(methylselanyl)phenyl)-N-methylquinazolin-4-amine (6d)

White soild, yield: 50%. mp: 164.3°C -165.3°C. ^{1}H NMR (400 MHz, $CDCl_3$) δ 7.77 (d, *J* = 6.6 Hz, 1H), 7.61 (s, 1H), 7.24 (d, *J* = 12.6 Hz, 2H), 7.10 (d, *J* = 6.2 Hz, 1H), 7.03 (dd, *J* = 15.4, 8.0 Hz, 2H), 3.62 (s, 3H), 2.37 (s, 3H). ^{13}C NMR (101 MHz, $CDCl_3$) δ 162.71 (s), 156.52 (s), 153.08 (s), 145.70 (s), 134.84 (s), 133.06 (s), 132.06 (s), 129.49 (s), 127.96 (s), 126.61 (s), 126.15 (s), 125.56 (s), 124.90 (s), 114.76 (s), 42.94 (s), 6.58 (s). ESI-MS (*m/z*) 398.0 $[M+H]^+$; HRMS (ESI) (*m/z*) $[M+H]^+$ calcd for $C_{16}H_{13}Cl_2N_3Se$, 397.9720; found, 397.9728. Purity: 95.6% (by HPLC).

2-chloro-N-methyl-N-(2-methyl-4-(methylselanyl)phenyl)quinazolin-4-amine (6f)

White soild, yield: 59%. mp: 104.6°C -105.3°C. 1H NMR (400 MHz, CDCl3) δ 7.66 (d, J = 8.3 Hz, 1H), 7.49 (t, J = 7.6 Hz, 1H), 7.30 (s, 1H), 7.21 (d, J = 9.9 Hz, 1H), 6.96 (d, J = 8.3 Hz, 1H), 6.92 (d, J = 7.6 Hz, 1H), 6.72 (d, J = 8.6 Hz, 1H), 3.45 (s, 3H), 2.33 (s, 3H), 2.07 (s, 3H). 13C NMR (101 MHz, CDCl3) δ 160.94 (s), 155.60 (s), 151.81 (s), 142.31 (s), 134.74 (s), 131.98 (s), 131.73 (s), 131.59 (s), 128.19 (s), 126.95 (s), 126.76 (s), 124.37 (s), 124.05 (s), 113.72 (s), 40.88 (s), 16.66 (s), 6.11 (s). ESI-MS (*m/z*) 378.0 $[M+H]^+$; HRMS (ESI) (*m/z*) $[M+H]^+$ calcd for $C_{17}H_{16}ClN_3Se$, 378.0271; found, 378.0269. Purity: 95.4% (by HPLC).

General procedure for the preparation of 6c, 6e, 6g, 6h, 6i

For the preparation of **6c** and **6g**, intermediates **4c** or **4g** (218 mg, 1 mmol), 2, 4-dichloroquinazoline (199 mg, 1 mmol) and NaAc (246 mg 3 mmol) were added to the solution of THF/H_2O (1/1, 18ml), and stirred at 60□ for 3 h. The mixture was diluted with H_2O and ethyl acetate after the reaction completed. The organic layer was separated, washed with brine, dried over Na_2SO_4, and evaporated to give an amber residue, which was subjected to silica gel chromatography (petroleum ether: ethyl acetate=10:1) to obtain **6c** and **6g**. For the preparation of **6e**, **6h** and **6i**, the mixture of **4e** or **4h**, **4i** (1 mmol), 2, 4-dichloroquinazoline (199 mg, 1 mmol) and NaH (60%, 60 mg, 1.5 mmol) in DMF (15ml) was stirred at 0□ for 4 h.

View Article Online
DOI: 10.1039/C8OB00875B

2-chloro-N-(3-fluoro-4-(methylselanyl)phenyl)-N-methylquinazolin-4-amine (6c)

White soild, yield: 74%. mp: 159.1°C -160.0°C. ^{1}H NMR (400 MHz, $CDCl_3$) δ 7.78 (d, *J* = 8.2 Hz, 1H), 7.62 (t, *J* = 7.1 Hz, 1H), 7.35 (t, *J* = 6.6 Hz, 1H), 7.17 – 7.08 (m, 1H), 7.05 (d, *J* = 8.4 Hz, 1H), 6.92 (dd, *J* = 11.4, 9.6 Hz, 2H), 3.62 (d, *J* = 14.6 Hz, 3H), 2.36 (d, *J* = 14.3 Hz, 3H). ^{13}C NMR (101 MHz, $CDCl_3$) δ 162.83 (d, *J* = 11.0 Hz), 160.33 (s), 156.54 (s), 153.11 (s), 147.07 (d, *J* = 9.2 Hz), 133.09 (s), 132.25 (d, *J* = 5.1 Hz), 127.99 (s), 126.11 (s), 125.56 (s), 122.25 (d, *J* = 3.0 Hz), 117.78 (d, *J* = 22.3 Hz), 114.86 (s), 113.02 (d, *J* = 24.4 Hz), 42.80 (s), 6.29 (s). ESI-MS (*m/z*) 382.1 $[M+H]^+$; HRMS (ESI) (*m/z*) $[M+H]^+$ calcd for $C_{16}H_{13}ClFN_3Se$, 382.0018; found, 382.0026. Purity: 99.6% (by HPLC).

N-(3-bromo-4-(methylselanyl)phenyl)-2-chloro-N-methylquinazolin-4-amine (6e)

White soild, yield: 85%. mp: 195.6°C -196.3°C. ^{1}H NMR (400 MHz, $CDCl_3$) δ 7.77 (dd, *J* = 8.2, 3.8 Hz, 1H), 7.65 – 7.57 (m, 1H), 7.44 – 7.39 (m, 1H), 7.19 (d, *J* = 8.4 Hz, 1H), 7.11 (ddd, *J* = 6.9, 5.4, 1.2 Hz, 1H), 7.08 – 7.02 (m, 2H), 3.61 (dd, *J* = 2.8, 1.0 Hz, 3H), 2.36 (s, 3H). ^{13}C NMR (101 MHz, $CDCl_3$) δ 162.69 (s), 156.52 (s), 153.10 (s), 145.64 (s), 134.49 (s), 133.06 (s), 129.83 (s), 129.32 (s), 127.97 (s), 126.16 (s), 125.57 (s), 125.44 (s), 124.58 (s), 114.76 (s), 42.98 (s), 7.48 (s). ESI-MS (*m/z*) 443.9 $[M+H]^+$; HRMS (ESI) (*m/z*) $[M+H]^+$ calcd for $C_{16}H_{13}BrClN_3Se$, 441.9215; found, 441.9217. Purity: 99.0% (by HPLC).

2-chloro-N-(2-fluoro-4-(methylselanyl)phenyl)-N-methylquinazolin-4-amine (6g)

Yellow oil, yield: 45%. ^{1}H NMR (400 MHz, $CDCl_3$) δ 7.70 (d, *J* = 8.3 Hz, 1H), 7.53 (t, *J* = 7.2 Hz, 1H), 7.16 – 7.12 (m, 1H), 7.11 (d, *J* = 3.2 Hz, 1H), 7.04 (d, *J* = 7.8 Hz, 1H), 7.01 (d, *J* = 7.2 Hz, 1H), 6.96 (d, *J* = 8.3 Hz, 1H), 3.50 (s, 3H), 2.33 (s, 3H). ^{13}C NMR (101 MHz, $CDCl_3$) δ 162.84 (s), 158.68 (s), 156.28 (d, *J* = 25.8 Hz), 152.90 (s), 134.01 (d, *J* = 6.6 Hz), 133.00 (s), 132.26 (d, *J* = 11.9 Hz), 128.72 (d, *J* = 25.6 Hz), 127.96 (s), 126.46 (d, *J* = 3.6 Hz), 125.60 (s), 124.89 (s), 118.17 (d, *J* = 21.3 Hz), 114.76 (s), 41.93 (s), 7.24 (s). ESI-MS (*m/z*) 382.0 $[M+H]^+$; HRMS (ESI) (*m/z*) $[M+H]^+$ calcd for $C_{16}H_{13}ClFN_3Se$, 382.0018; found, 382.0010. Purity: 99.1% (by HPLC).

View Article Online
DOI: 10.1039/C8OB00875B

2-chloro-N-(2-chloro-4-(methylselanyl)phenyl)-N-methylquinazolin-4-amine (6h)

White soild, yield: 44%. mp: 117.1°C -117.9°C. ^{1}H NMR (400 MHz, $CDCl_3$) δ 7.76 (d, *J* = 8.3 Hz, 1H), 7.59 (t, *J* = 7.6 Hz, 1H), 7.53 (d, *J* = 1.6 Hz, 1H), 7.31 (dd, *J* = 8.2, 1.7 Hz, 1H), 7.09 (d, *J* = 8.1 Hz, 1H), 7.06 (d, *J* = 7.4 Hz, 1H), 6.87 (d, *J* = 8.5 Hz, 1H), 3.54 (s, 3H), 2.42 (s, 3H). ^{13}C NMR (101 MHz, $CDCl_3$) δ 162.50 (s), 156.48 (s), 152.87 (s), 141.78 (s), 134.23 (s), 132.93 (s), 132.69 (s), 131.47 (s), 129.67 (s), 129.24 (s), 127.92 (s), 125.68 (s), 124.85 (s), 114.82 (s), 41.53 (s), 29.72 (s). ESI-MS (*m/z*) 397.9 $[M+H]^+$; HRMS (ESI) (*m/z*) $[M+H]^+$ calcd for $C_{16}H_{13}Cl_2N_3Se$, 397.9720; found, 397.9721. Purity: 95.9% (by HPLC).

N-(2-bromo-4-(methylselanyl)phenyl)-2-chloro-N-methylquinazolin-4-amine (6i)

White soild, yield: 70%. mp: 116.9°C -117.4°C. ^{1}H NMR (400 MHz, $CDCl_3$) δ 7.67 (d, *J* = 8.3 Hz, 1H), 7.64 (s, 1H), 7.51 (t, *J* = 7.5 Hz, 1H), 7.28 (d, *J* = 7.7 Hz, 1H), 7.02 (d, *J* = 8.0 Hz, 1H), 6.98 (d, *J* = 7.6 Hz, 1H), 6.78 (d, *J* = 8.5 Hz, 1H), 3.45 (s, 3H), 2.34 (s, 3H). ^{13}C NMR (101 MHz, $CDCl_3$) δ 162.28 (s), 156.46 (s), 152.86 (s), 143.25 (s), 134.57 (s), 134.55 (s), 132.91 (s), 130.38 (s), 129.38 (s), 127.88 (s), 125.70 (s), 124.98 (s), 123.02 (s), 114.80 (s), 41.70 (s), 7.35 (s). ESI-MS (*m/z*) 443.9 $[M+H]^+$; HRMS (ESI) (*m/z*) $[M+H]^+$ calcd for $C_{16}H_{13}BrClN_3Se$, 441.9215; found, 441.9213. Purity: 97.6% (by HPLC).

General procedure for the preparation of 7a

A solution of **6a** (2-chloro-N-methyl-N-(4-(methylselanyl)phenyl)quinazolin-4-amine, 363 mg, 1 mmol) in CH_3OH (20ml) containing of NaOH (120 mg, 3 mmol) was heated at 70 for 3 h. The solvent was evaporated to give an amber residue, which was further purify by silica gel chromatography (petroleum ether: ethyl acetate=10:1) to give **7a**.

2-methoxy-N-methyl-N-(4-(methylselanyl)phenyl)quinazolin-4-amine (7a)

Yellow oil, yield: 52%. ^{1}H NMR (400 MHz, $CDCl_3$) δ 7.65 (d, *J* = 8.3 Hz, 1H), 7.48 (t, *J* = 7.6 Hz, 1H), 7.40 (s, 1H), 7.38 (s, 1H), 7.08 (s, 1H), 7.05 (s, 1H), 7.02 (d, *J* = 8.4 Hz, 1H), 6.88 (t, *J* = 7.7 Hz, 1H), 4.10 (s, 3H), 3.59 (s, 3H), 2.37 (s, 3H). ^{13}C NMR (101 MHz,

View Article Online
DOI: 10.1039/C8OB00875B

$CDCl_3$) δ 164.16 (s), 162.15 (s), 153.49 (s), 146.46 (s), 132.24 (s), 131.58 (s), 129.96 (s), 126.98 (s), 126.56 (s), 122.52 (s), 113.93 (s), 54.40 (s), 42.67 (s), 7.36 (s). ESI-MS (*m/z*) 360.1 $[M+H]^+$; HRMS (ESI) (*m/z*) $[M+H]^+$ calcd for $C_{17}H_{17}N_3OSe$, 360.0610; found, 360.0609. Purity: 99.8% (by HPLC).

General procedure for the preparation of 9

4-bromo-2H-chromen-2-one (**9**) was synthesized according to literature method.[1]

4-bromo-2H-chromen-2-one (9)

White soild, yield: 80%. ^1H NMR (400 MHz, $CDCl_3$) δ 7.83 (dt, *J* = 8.0, 4.1 Hz, 1H), 7.60 (dt, *J* = 8.4, 4.2 Hz, 1H), 7.42 – 7.29 (m, 2H), 6.85 (d, *J* = 8.0 Hz, 1H). ^{13}C NMR (101 MHz, $CDCl_3$) δ 158.61 (s), 152.44 (s), 141.44 (s), 133.21 (s), 128.01 (s), 124.96 (s), 119.54 (s), 118.89 (s), 116.97 (s).

General procedure for the preparation of 10

To a solution of 4-bromo-2H-chromen-2-one (**9**, 224 mg, 1 mmol) and 2, 4-dichloroquinazoline (199 mg, 1 mmol) in 20 mL DMF, DIPEA (193.5 mg, 1.5 mmol) was added and the mixture was stirred at 110 overnight. After cooled to the room temperature, the reaction mixture was diluted with H_2O and ethyl acetate. The organic layers was filtered, washed with brine and dried over Na_2SO_4. Evaporation of the solvent to get the crude product which was purified by silica gel chromatography (petroleum ether: ethyl acetate=10:1) to afford 4-(methyl(4-(methylselanyl)phenyl)amino)-2H-chromen-2-one (**10**).

4-(methyl(4-(methylselanyl)phenyl)amino)-2H-chromen-2-one (10)

Brown solid, yield: 49%. mp: 109.6°C -110.3°C. ^1H NMR (400 MHz, $CDCl_3$) δ 7.36 (d, *J* = 7.9 Hz, 3H), 7.29 (s, 1H), 6.99 (d, *J* = 7.9 Hz, 3H), 6.89 (t, *J* = 7.3 Hz, 1H), 5.90 (s, 1H), 3.38 (s, 3H), 2.35 (s, 3H). ^{13}C NMR (101 MHz, $CDCl_3$) δ 162.58 (s), 156.97 (s), 154.15 (s),

View Article Online
DOI: 10.1039/C8OB00875B

146.48 (s), 131.61 (s), 131.05 (s), 129.13 (s), 126.63 (s), 125.29 (s), 122.94 (s), 117.58 (s), 115.94 (s), 97.71 (s), 43.64 (s), 7.44 (s). ESI-MS (*m/z*) 346 $[M+H]^+$; HRMS (ESI) (*m/z*) $[M+H]^+$ calcd. for $C_{17}H_{15}NO_2Se$, 346.0341; found, 346.0338. Purity: 96.7% (by HPLC).

Cell Lines and Culture Conditions

The human cancer cell lines (A549, HeLa, HEPG2, RKO, LOVO, HCT116) used in this study were purchased from the Laboratory Animal Service Center at Sun Yat-sen University (Guangzhou, China). Human cancer cell lines A549, HeLa, HEPG2, RKO were cultivated in DMEM containing 10% (v/v) heat-inactivated fetal bovine serum (FBS), 100 units/mL penicillin, and 100 μg/mL streptomycin, respectively. Human cancer cell lines HCT-116 were cultivated in RPMI 1640 medium containing 10% (v/v) heat-inactivated FBS, 100 units/ mL penicillin, and 100 mg/mL streptomycin, respectively. The cells were incubated at 37 ^oC under a 5% CO_2 and 90% relative humidity (RH) atmosphere.

MTT assay. Cells grown to the logarithmic phase were seeded 5×10^3 -10×10^3 cells/well into 96-well plates (Nest Biotechnology Co.,Ltd.) for 24 h, and then exposed to different concentrations of the test compounds for 48 h. After attached cells were incubated with 5 mg/mL MTT (Sigma, USA) for another 4 h, the suspension was discarded, and subsequently the dark blue crystals (formazan) were solubilized in dimethyl sulfoxide (DMSO). The absorbance of the solution at 570 nm was measured using a multifunction microplate reader (Molecular Devices, Flex Station 3), and each experiment was performed at least in triplicate. IC50 values, which the drug concentrations required to cause 50% cancer cell growth inhibition, were used to express the cytotoxic effects of each compound and were calculated with GraphPad Prism Software version 5.02 (GraphPad Inc., La Jolla, CA, USA).

In vitro tubulin polymerization assay. A tubulin polymerization assay was performed by measuring the increase in fluorescence intensity, which can be easily recorded due to the incorporation of a fluorescent reporter, DAPI (4',6-diamidino-2-phenylindole), a fluorophore that is known to be a DNA intercalator. A commercial kit (cytoskeleton, cat. #BK011P) purchased from Cytoskeleton (Danvers, MA, USA) was used for the tubulin polymerization. The final buffer used for tubulin polymerization contained 80.0 mM piperazine-N, N′ -bis(2-ethanesulfonic acid) sequisodium salt (pH 6.9), 2.0 mM MgCl2,

View Article Online
DOI: 10.1039/C8OB00875B

0.5 mM EGTA, 1 mM GTP, and 10.2% glycerol. First, 5 μL of the tested compounds at the indicated concentrations was added, and the mixture was warmed to 37 °C for 1 min; then, the reaction was initiated by the addition of 55 μL of the tubulin solution. The fluorescence intensity enhancement was recorded every 60 sec for 90 min in a multifunction microplate reader (Molecular Devices, Flex Station 3) (emission wavelength of 410 nm, excitation wavelength of 340 nm). The area under the curve was used to determine the concentration that inhibited tubulin polymerization by 50% (IC_{50}) and was calculated using GraphPad Prism Software version 5.02 (GraphPad Inc., La Jolla, CA, USA).

Immunofluorescence microscopy. In a 10 mm confocal culture dish, 1×10^4 cells were grown for 24 h and then incubated in the presence/absence of compound **5a** at the indicated concentrations for another 8 h. After being washed with phosphate-buffered solution (PBS) and fixed in 4% pre-warmed (37°C) paraformaldehyde for 15 min, the cells were permeabilized with 0.5% Triton X-100 for 15 min and blocked for 30 min in 10% goat serum. Then, the cells were incubated with mouse anti-tubulin antibody (CST, USA) at 4°C overnight, washed with PBS three times, and incubated with goat anti-mouse IgG/Alexa-Fluor 488 antibody (Invitrogen, USA) for 1 h. The samples were immediately visualized on a Zeiss LSM 570 laser scanning confocal microscope (Carl Zeiss, Germany) after the nuclei were stained with Hoechst 33342 (Sigma, USA) in the dark at room temperature for 30 min.

Cell cycle analysis. HELA cells were seeded in 6-well plates (3×10^5 cells/well), incubated in the presence/absence of compound **5a** at the indicated concentrations for 12 or 24 h, harvested by centrifugation, and then fixed in ice-cold 70% ethanol overnight. After the ethanol was removed the next day, the cells were re-suspended in ice-cold PBS, treated with RNAse A (Keygen Biotech, China) at 37°C for 30 min, and then incubated with the DNA staining solution propidium iodide (PI, Keygen Biotech, China) at 4°C for 30 min. Approximately 10,000 events were detected by flow cytometry (Beckman Coulter, Epics XL) at 488 nm. The data regarding the number of cells in different phases of the cell cycle were analysed using EXPO32 ADC analysis software.

Apoptosis analysis. The preparation of the HELA cell sample was the same as for the cell cycle analysis. After incubation, cells were harvested and incubated with 5 μL of Annexin-V/FITC (Keygen Biotech, China) in binding buffer (10 mM HEPES, 140 mM NaCl, and

View Article Online
DOI: 10.1039/C8OB00875B

2.5 mM $CaCl_2$ at pH 7.4) at room temperature for 15 min. PI solution was then added to the medium for another 10 min-incubation. Almost 10,000 events were collected for each sample and analysed by flow cytometry (Beckman Coulter, Epics XL). The percentage of apoptotic cells was calculated using EXPO32 ADC Analysis software.

Mitochondrial membrane potential and ROS accumulation assay. A lipophilic cationic dye, 5,5′,6,6′-tetrachloro-1,1′,3,3′-tetraethyl-benzimidazolcarbocyanine (JC-1, Beyotime, China) was used to monitor the level of MMP in the cells. At normal state, the MMP is high and JC-1 appears as aggregates, which indicated by red fluorescence. However, when apoptosis occurs, the MMP reduced and JC-1 displayed as monomers, which indicated by green fluorescence. We applied two methods which including flow cytometry and fluorescence microscopy to detect the MMP. For flow cytometry analysis, HELA cells were plated in 6-well plates (3×10^5 cells/well) and grown for 24 h, and treated with compounds **5a** at the indicated concentrations for 24 h. Then the cells were harvested by centrifugation and incubated with JC-1 solution for 30 min. After briefly washing, the proportion of green and red fluorescence intensity were immediately detected and analysed by flow cytometry. For the fluorescence microscopy detection, HELA cells were plated in a confocal culture dish at 5×10^4 cells/dish and grown for 24 h, and treated with compound **5a** at the indicated concentrations for another 24 h. Then the cells were stained with 2 μM JC-1 at 37 °C for 30 min, washed with PBS and then the cell nuclei were stained with Hoechst 33342 (Sigma, USA) for 10 min in the dark. The cell images were immediate detected by a Zeiss LSM 570 laser scanning confocal microscope (Carl Zeiss, Germany).

Intracellular ROS accumulation assay was performed by fluorescence microscopy using the Reactive Oxygen Species Assay Kit (ROS Assay Kit, Beyotime). HELA cells were cultured in 6-well plates (3×10^5 cells/well) for 24 h. After adding compound **5a** for 12 h, the culture supernatants were removed, and the cells were then incubated with 10 mM DCFH-DA in fresh medium at 37 °C for 30 min. After incubation, the culture medium was removed, and the cells were washed with PBS buffer three times. The production of ROS could be measured by changes in the fluorescence intensity due to the intracellular accumulation of dichlorofluorescein (DCF) caused by the oxidation of DCFH. The intracellular ROS level, as indicated by the DCF fluorescence, was determined by measuring the fluorescence intensity on a multifunctional monochromator-based microplate reader with the excitation and emission wavelengths set at 488 and 525 nm, respectively. To observe the intracellular ROS level visually, we used the Arrayscan VTI High Content Analysis System to acquire

View Article Online
DOI: 10.1039/C8OB00875B

cell images after the cell nuclei were stained with Hoechst 33342 (Sigma) for 10 min in dark conditions.

Reference

1. R. L. Siegel, K. D. Miller, A. Jemal, Cancer statistics, CA: *Cancer J. Clin.*, 2015, **65**, 5–29.

2. R. Siegel, C. DeSantis, K. Virgo, K. Stein, A. Mariotto, T. Smith, et al., Cancer treatment and survivorship statistics, CA: *Cancer J. Clin.*, 2012, **62**, 220– 241.

3. W. Chen, Cancer statistics: updated cancer burden in China, Chin. *J. Cancer Res.,* 2015, **27**, 1.

4. C. H. Aylett, J. Lowe, L. A. Amos, New insights into the mechanisms of cytomotive actin and tubulin filaments, *Int. Rev. Cell. Mol. Biol.,* 2011, **292**, 1- 71.

5. P. K. Sorger, M. Dobles, R. Tournebize, A. A. Hyman, Coupling cell division and cell death to microtubule dynamics, *Curr. Opin. Cell Biol*., 1997, **9**, 807-814.

6. T. Horio, T. Murata, The role of dynamic instability in microtubule organization, *Front. Plant Sci.,* 2014, **5**, 511.

7. M. Kavallaris, Microtubules and resistance to tubulin-binding agents, *Nat. Rev. Cancer*, 2010, **10**, 194-204.

8. F. Pellegrini, D. R. Budman, Review: tubulin function, action of antitubulin drugs, and new drug development, *Cancer Invest.*, 2005, **23**, 264-273.

9. P. B. Schiff, J. Fant, S. B. Horwitz, Promotion of microtubule assembly in vitro by taxol, *Nature*, 1979, **277**, 665-667.

10. B. Bhattacharyya, D. Panda, S. Gupta, M. Banerjee, Anti-mitotic activity of colchicine and the structural basis for its interaction with tubulin, *Med. Res. Rev.*, 2008, **28**, 155−183.

11. N. Sirisoma, K. Kasibhatla, A. Pervin, H. Zhang, S. Jiang, Cai Discovery of 2-chloro-**N**-(4-methoxyphenyl)-**N**-methylquinazolin-4-amine (EP128265, MPI-0441138) as a potent inducer of apoptosis with high in vivo activity, *J. Med. Chem.*, 2008, **51**, 4771-4779.

12. K S. Prabhu, X. G. Lei, Selenium, *Adv. Nutr.*, 2016, **7**, 415-417.

View Article Online
DOI: 10.1039/C8OB00875B

13. G. V. Kryukov, S. Castellano, S. V. Novoselov, A. V. Lobanov, O. Zehtab, R. Guigó, V. N. Gladyshev, Characterization of Mammalian Selenoproteomes, *Science,* 2003, **300**, 1439-1443.

14. Anonymous. Observations on effect of sodium selenite in prevention of Keshan disease. *Chin. Med. J.*, 1979, **92**, 471–476,

15. R. Moreno-Reyes, D. Egrise, J. Nève, J. L. Pasteels, A. Schoutens, Selenium deficiency-induced growth retardation is associated with an impaired bone metabolism and osteopenia. *J. Bone Miner. Res.*, 2001, **16**,1556–1563.

16. U. Ahsan, Z. Kamran, I. Raza, S. Ahmad, W. Babar, M. H. Riaz, Z. Iqbal, Role of selenium in male reproduction - a review. *Anim. Reprod. Sci.*, 2014, **146**, 55–62.

17. M. Vinceti, C. M. Crespi, C. Malagoli, C. Del Giovane, V. Krogh, The current epidemiologic evidence on selenium and human cancer risk, *J. Environ. Sci. Health C Environ. Carcinog Ecotoxicol Rev.,* 2013, **31**, 305-341.

18. A. K. Sharma, S. Amin, Post Select: selenium on trial, *Future Med. Chem*., 2013, **5**, 163-174.

19. G. V. Kryukov, S. Castellano, S. V. Novoselov, A. V. Lobanov, O. Zehtab, Characterization of Mammalian Selenoproteomes. *Science*, 2003, **300**, 1439−1443.

20. A. A. Turanov, R. A. Everley, S. Hybsier, K. Renko, L. Schomburg, S. P. Gygi, D. L. Hatfield, V. N. Gladyshev, Regulation of selenocysteine content of human selenoprotein P by dietary selenium and insertion of cysteine in place of selenocysteine, *PLoS One*, 2015.**10**, e0140353.

21. M.P. Rayman, Selenium in cancer prevention: A review of the evidence and mechanism of action. *Proc. Nutr. Soc.*, 2005, **64**, 527–542.

22. Y. Yang, F. Huang, Y. Ren, L. Xing, Y. Wu, Z. Li, H. Pan, C. Xu, The anticancer effects of sodium selenite and selenomethionine on human colorectal carcinoma cell lines in nude mice. *Oncol. Res.* 2009, **18**, 1- 8.

23. C. Y. Chung, S. V. Madhunapantula, D. Desai, S. Amin, G. P. Robertson, Melanoma prevention using topical PBISe, *Cancer Prev. Res.*, 2011, **4**, 935-948.

24. T. Lin, Z. Ding, N. Li, J. Xu, G. Luo, J. Liu, J. Shen, Seleno-cyclodextrin sensitises

View Article Online
DOI: 10.1039/C8OB00875B

human breast cancer cells to TRAIL-induced apoptosis through DR5 induction and NF-kappaB suppression, *Eur. J. Cancer*, 2011, **47**, 1890 -1907.

25. N. Nguyen, A. Sharma, N. Nguyen, A. K. Sharma, D. Desai, S J. Huh, S. Amin, C. Meyers, G. P. Robertson, Melanoma chemoprevention in skin reconstructs and mouse xenografts using isoselenocyanate-4, *Cancer Prev. Res.*, 2011, **4**, 248 - 258.

26. H. Zeng, W. H. Cheng, L. K. Johnson, Methylselenol, a selenium metabolite, modulates p53 pathway and inhibits the growth of colon cancer xenografts in Balb/c mice. *J. Nutr. Biochem.*, 2013, **24**, 776 - 780.

27. E. A. Santos, E. Hamel, R. Bai, J. C. Burnett, C. S. S. Tozatti, D. Bogo, R. T Perdomo, A. M. M. Antunes, M. M. Marques, M. F. C. Matos, D. P. Lima, Synthesis and evaluation of diaryl sulfides and diaryl selenide compounds for antitubulin and cytotoxic activity. *Bioorg. Med. Chem. Lett.*, 2013, **23**, 4669 - 4673.

28. Q. Guan, F. Yang, D. Guo, J. Xu, M. Jiang, C. Liu, K. Bao, Y. Wu, W. Zhang, Synthesis and biological evaluation of novel 3,4-diaryl-1,2,5-selenadiazol analogues of combretastatin A-4, *Eur. J. Med. Chem.*, 2014, **87**, 1 - 9.

29. D. Plano, D. N. Karelia, M. K. Pandey, J. E. Spallholz, S. Amin, A. K. Sharma, Design, synthesis, and biological evaluation of novel selenium (Se-NSAID) molecules as anticancer agents, *J. Med. Chem.*, 2016, **59**, 1946 - 1959.

30. An. Baijiao , Synthesis and Biological Evaluation of Selenium-Containing 4‑Anilinoquinazoline Derivatives as Novel Antimitotic Agents. *J. Med. Chem.*, 2018, **61**, 2571‑2588.

31. P. R. Clarke, L. A. Allan, Cell-cycle control in the face of damage-a matter of life or death, *Trends Cell Biol.*, 2009, **19**, 89–98.

32. J. C. Reed, Apoptosis-based therapies, *Nat. ReV. Drug DiscoVery*, 2002, **1**, 111-121.

33. S. W. Fesik, Promoting apoptosis as a strategy for cancer drug discovery, *Nat. Rev. Cancer*, 2005, **5**, 876–885.

34. K. Sinha, J. Das, P. B. Pal, P. C. Sil, Oxidative stress: the mitochondria-dependent and mitochondria-independent pathways of apoptosis, *Arch. Toxicol*, 2013, **87**, 1157-1180.

View Article Online
DOI: 10.1039/C8OB00875B

35. A. T. Dharmaraja, Role of reactive oxygen species (ROS) in therapeutics and drug resistance in cancer and bacteria. *J. Med. Chem.*, 2017, **60**, 3221-3240.